SUPPLEMENTARY SECTION

The intracellular domains of the EphB6 and EphA10 receptor tyrosine pseudokinases function as dynamic signalling hubs

Lung-Yu Liang[1,2], Michael Roy[1,2], Christopher R. Horne[1,2], Jarrod J. Sandow[1,2], Minglyanna Surudoi[1], Laura Dagley[1,2], Samuel N. Young[1], Toby Dite[2], Jeffrey J. Babon[1,2], Peter W. Janes[3], Onisha Patel[1,2*], James M. Murphy[1,2*], Isabelle S. Lucet[1,2*]

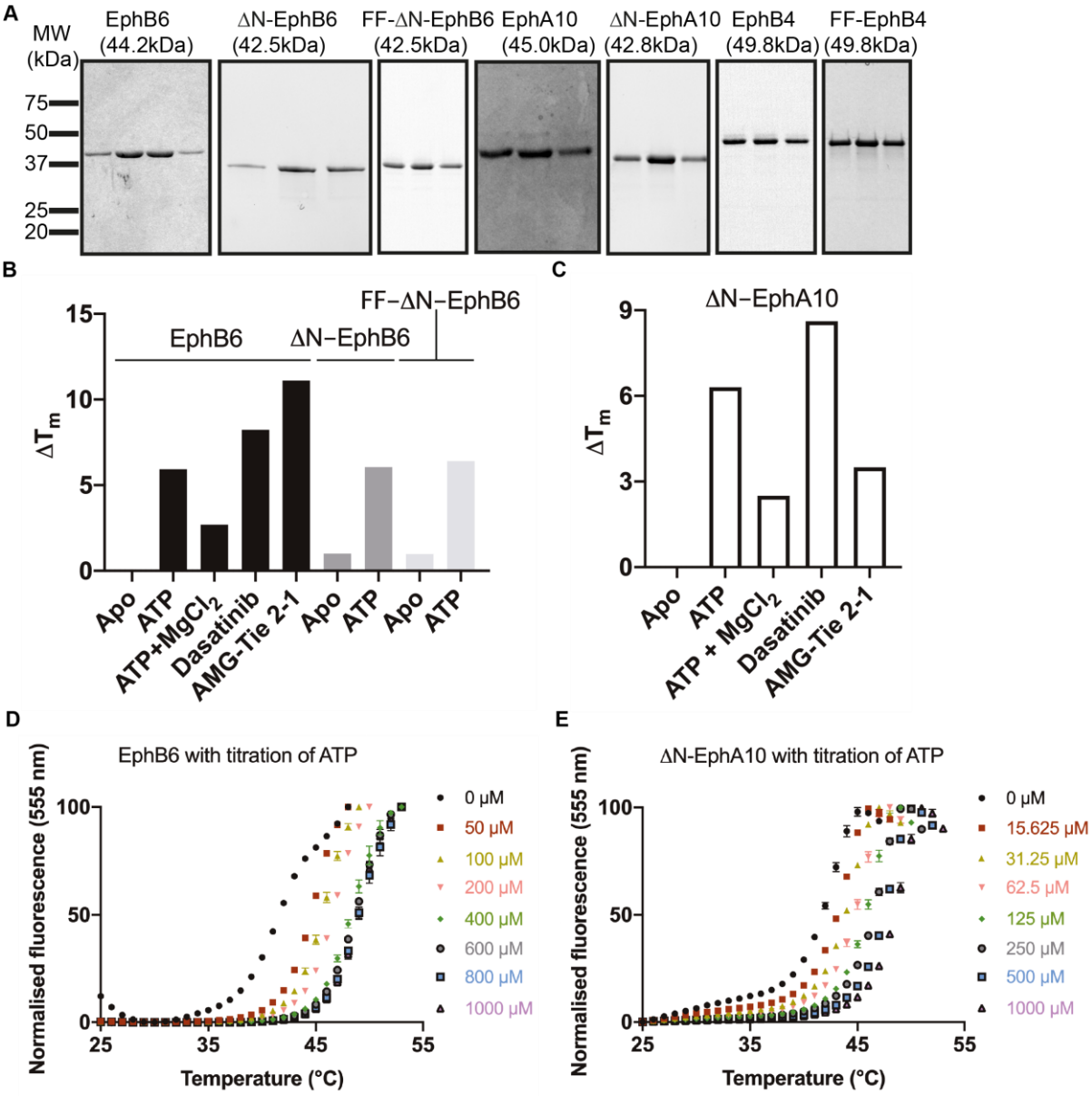

Supplementary Figure 1: Purification of Eph receptor intracellular domains and their abilities to bind nucleotides/kinase inhibitors

(A) Reducing SDS-PAGE of fractions from the gel filtration peak of recombinant proteins of the Eph receptor intracellular domains used in this study. (B) Thermal shift assays were used to assess the binding of ATP at 200μM in the presence/absence of 1mM Mg^{2+}, 40μM type I (Dasatinib) and 40μM type II (AMG-Tie 2-1) kinase inhibitors to the EphB6 intracellular domains. (C) Thermal shift assays were used to assess the binding of ATP at 100μM (in the presence or absence of 0.5mM Mg^{2+}), 40μM type I (Dasatinib) and 40μM type II (AMG-Tie 2-1) kinase inhibitors to the EphA10 intracellular domains. Titrations of ATP for binding to EphB6 (D), ΔN-EphA10 (E).

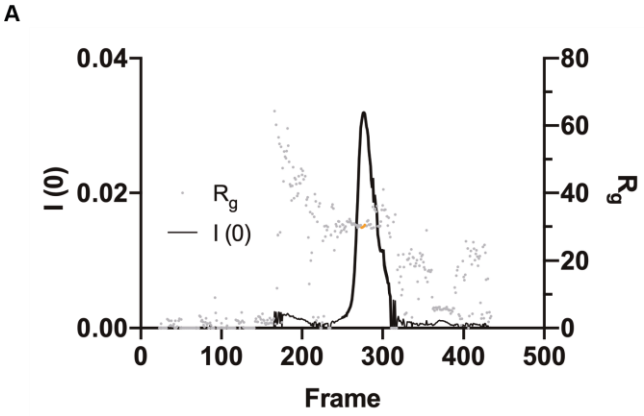

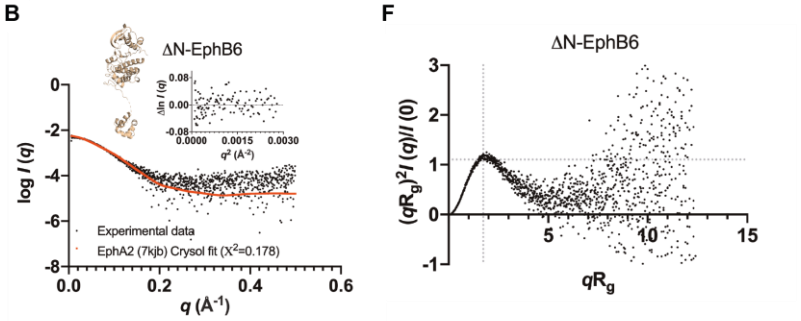

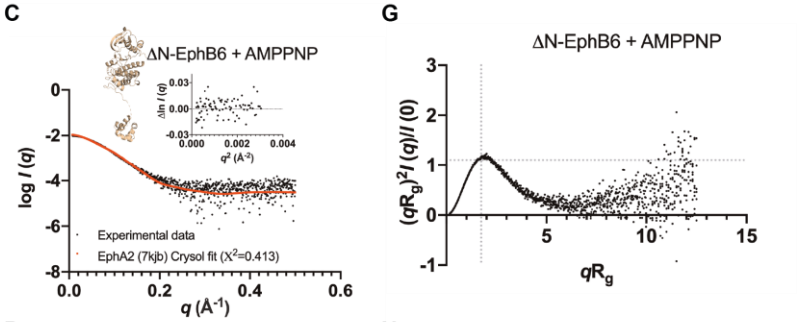

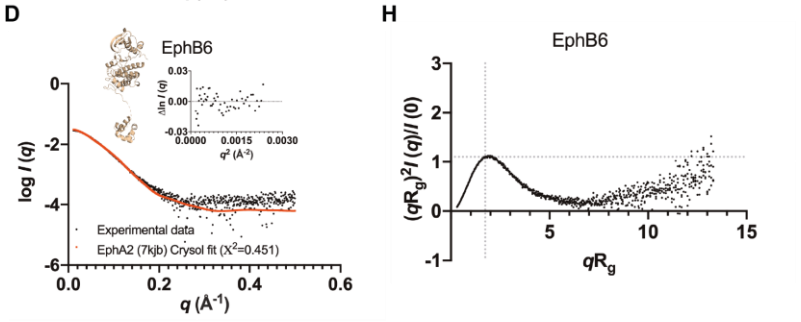

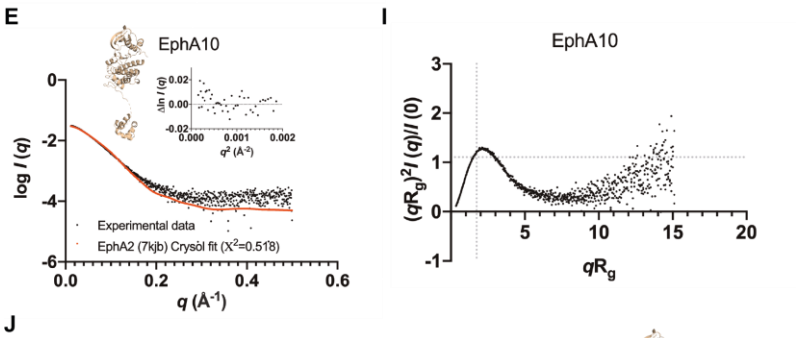

J

	χ^2 from EphB6 (residues 625-1021) (Alphafold)	χ^2 from EphA10 (residues 600-1008) (Alphafold)	χ^2 from EphA2 (7KJB)	χ^2 from EphA2 (7KJA)
EphB6 (residues 625-1021)	0.309	NA	0.451	9.156
ΔN-EphB6 (residues 643-1021)	0.129	NA	0.178	1.292
ΔN-EphB6 + AMPPNP (residues 643-1021)	0.130	NA	0.413	7.408
EphA10 (residues 600-1008)	NA	0.220	0.518	3.495

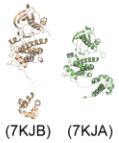

Supplementary Figure 2: In solution structural characterisation of EphB6 and EphA10 using small-angle X-ray scattering (SAXS)

(A) The scattering profile of EphA10 from an inline SEC-SAXS experiment. The R_g of the exposures selected for averaging and parameter estimation are highlighted in orange, while R_g of the flanking exposures are shown in grey. (B-E) The SAXS profiles compared to the theoretical scatter calculated from the EphA2 crystal structure coordinates (PDB: 7KJB) by CRYSOL for ΔN-EphB6 (χ^2=0.178) (B), ΔN-EphB6 + AMPPNP (χ^2=0.413) (C), EphB6 (χ^2=0.451) (D) and EphA10 (χ^2=0.518) (E). The residuals of Guinier plots (inset) are illustrative of monodispersed proteins in solution, free from aggregation and inter-particle interaction. (F-I) The dimensionless Kratky plots for ΔN-EphB6 (F), ΔN-EphB6 + AMPPNP (G), EphB6 (H) and EphA10 (I) show these recombinant proteins are globular and have folded domains. *I(0)* and R_g are calculated by Guinier analysis. The dotted lines at the X-axis mark 1.732, where a peak > 1.732 indicates flexibility of proteins. The dotted line at the Y-axis marks 1.104, where a peak >1.104 indicates asymmetry of proteins. (J) A table summarising the χ^2 values calculated from the EphB6 and EphA10 SAXS profiles compared to the theoretical scatter calculated from different structure models. NA: not applicable.

A

XL	EphB6 residues	EphA2 equivalents	CA (Å)	Motifs
DMTMM	E664:K740	E607:K684	9.8	C-JM:β4-β5
DMTMM	D666:K740	H609:K684	8.4	C-JM:β4-β5
DMTMM	K671:E735	T614:E679	14.1	β1:β4
DMTMM	E674:K1001	K617:R957	81.8	β1:SAM α5
DMTMM	E683:K1001	E626:R957	76.1	β2:SAM α5
DMTMM	E735:K810	E679:K754	15.5	β4:β8
DMTMM	E764:K1000	D708:K956	61.8	αD-αE:SAM α5
DMTMM	E764:K1001	D708:R957	58.3	αD-αE:SAM α5
DMTMM	K917:1020E	K873:P975	NA	αI:PBM
DMTMM	K917:1021-C'	K873:I976-C'	NA	αI:PBM
DMTMM	K1001:1020E	R957:P975	NA	SAM α5:PBM
BS^3	K900:K1001	Q856:R957	41.5	αH-αI:SAM α5
BS^3	K917:K1001	K873:R957	49.5	αJ:SAM α5

B

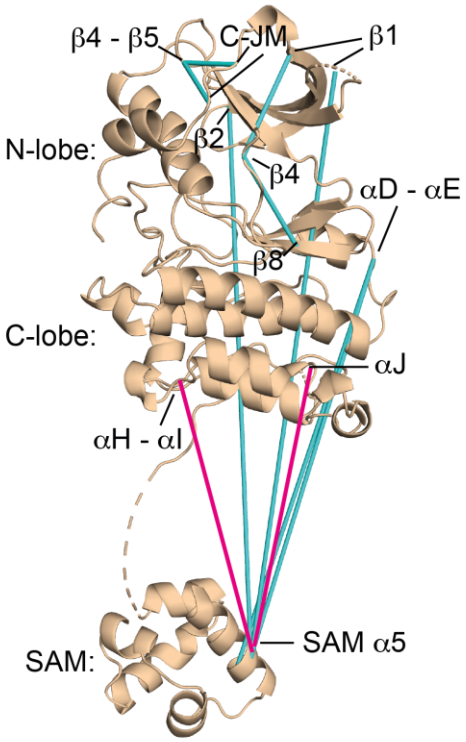

Supplementary Figure 3: EphB6 intracellular domains exhibit dynamic inter-domain interaction by chemical crosslinking-mass spectrometry experiments

(A) The amino acid residues crosslinked by DMTMM (0 Å spacer) are highlighted in cyan, and the amino acid residues crosslinked by BS^3 (11.4 Å spacer) are highlighted in magenta. The residue number of the amino acids of EphA2 equivalent to the cross-linked residues in EphB6, the distance of the backbone carbon and the secondary structures in the EphA2 crystal structure (PDB: 7KJB) are highlighted in light brown. The distances of CA of the three crosslinking events involving the PDZ domain-binding motif (PBM) were not calculated (NA: not applicable), because the EphA2 crystal structure does not contain the PBM. C′: the carboxylic end of proteins. (B) The amino acid residues in the EphA2 crystal structure (PDB: 7KJB) equivalent to the crosslinked residues in EphB6 are connected by cyan lines (crosslinked by DMTMM), and by magenta lines (crosslinked by BS^3).

A

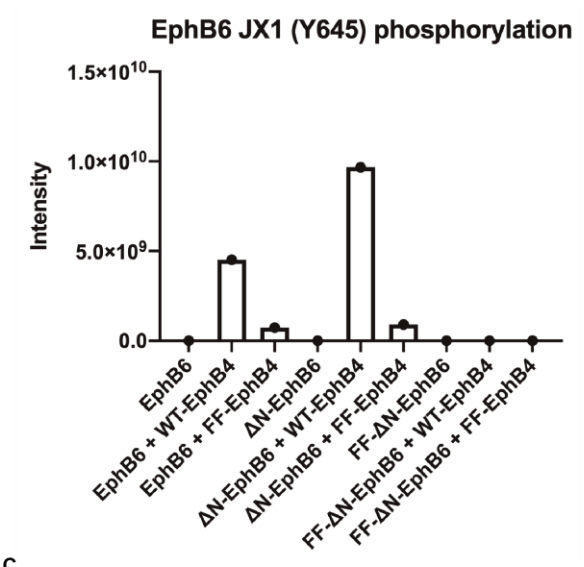

B

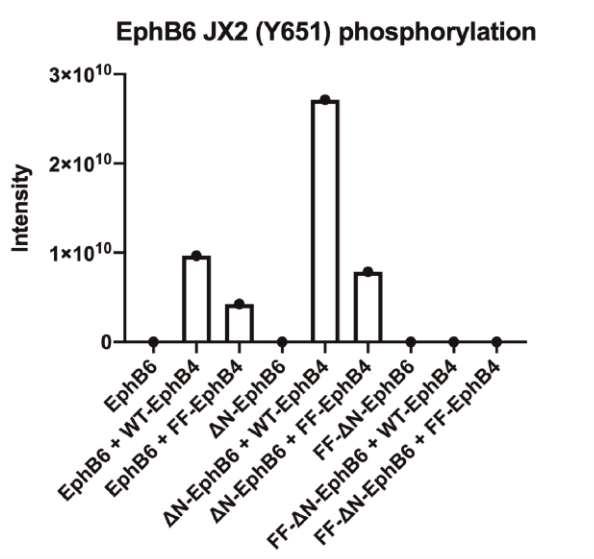

C

	Y644	Y645 (JX1)	Y651 (JX2)	Y669
EphB6	0.6	0.93	1	1
ΔN-EphB6	0.6	0.93	1	1
FF-ΔN-EphB6	N.D.	N.D.	N.D.	1

D

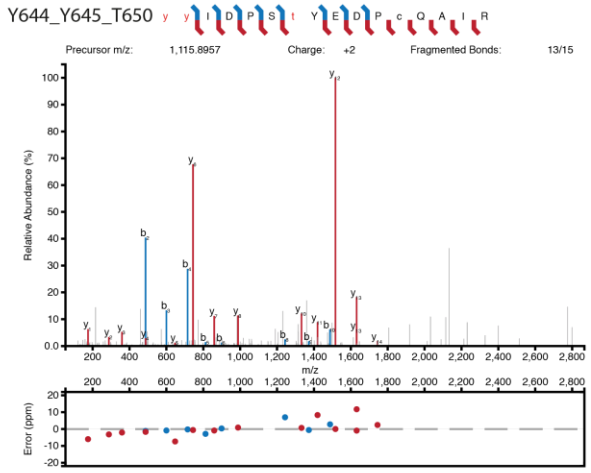

E

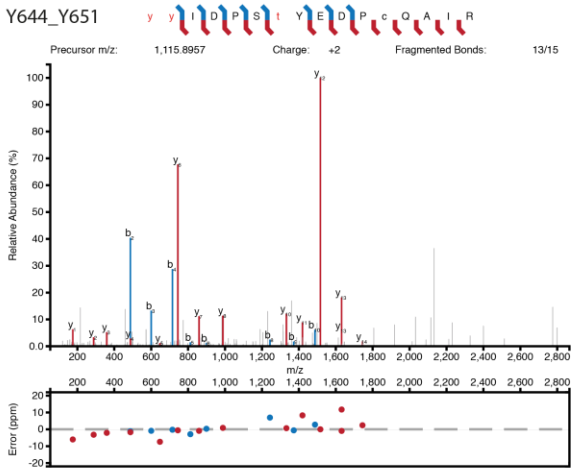

F

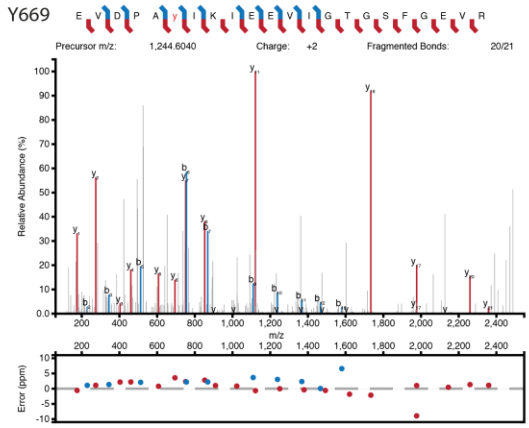

Supplementary Figure S4: Identification of phosphosites in recombinant EphB6 proteins by mass spectrometry

(A) pY645 (JX1) phosphorylation intensity in recombinant EphB6 protein from different *in vitro* kinase activity assays. (B) pY651 (JX2) phosphorylation intensity in recombinant EphB6 protein from different *in vitro* kinase activity assays. (C) Identification of the sites of WT-EphB4-mediated phosphorylation in recombinant EphB6, ΔN-EphB6 and FF-ΔN-EphB6 by mass spectrometry. The numbers in the table indicate the confidence of site identification by the mass spectrometry. A score of 1 indicates 100% confidence. The MS/MS spectra of peptides containing pY644 and pY645 (D), pY644 and pY651 (E) and pY699 (F) from P_L- and P_H-EphB6 recombinant proteins identified by mass spectrometry.

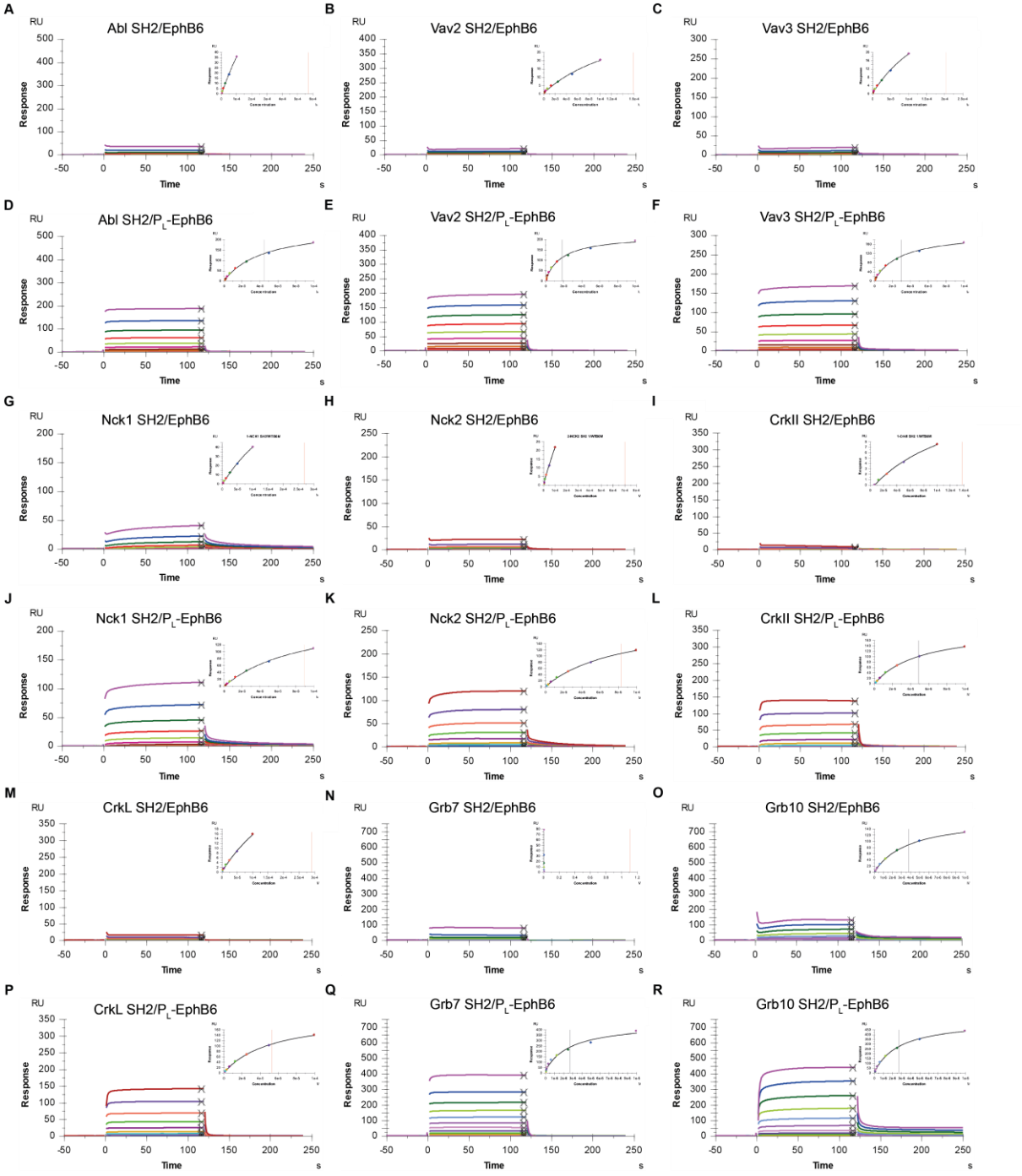

Supplementary Figure S5: Binding of SH2 domains to the non-phosphorylated EphB6 and phosphorylated recombinant protein (P_L-ΔN-EphB6) measured by surface plasmon resonance (SPR).

Binding of the SH2 domains of Abl (A), Vav2 (B), Vav3 (C) to non-phosphorylated ΔN-EphB6, and binding of the SH2 domains of Abl (D), Vav2 (E), Vav3 (F) to P_L-ΔN-EphB6. Binding of the SH2 domains of Nck1 (G), Nck2 (H), CrkII (I) to non-phosphorylated ΔN-EphB6, and binding of the SH2 domains of Nck1 (J), Nck2 (K), CrkII (L) to P_L-ΔN-EphB6. Binding of the

SH2 domains of CrkL (M), Grb7 (N), Grb10 (O) to non-phosphorylated ΔN-EphB6, and binding of the SH2 domains of CrkL (P), Grb7 (Q), Grb10 (R) to P_L-ΔN-EphB6. The immobilisation levels of ΔN-EphB6 and P_L-ΔN-EphB6 on the SA sensor chip were 1598.3 RU and 1064 RU, respectively.

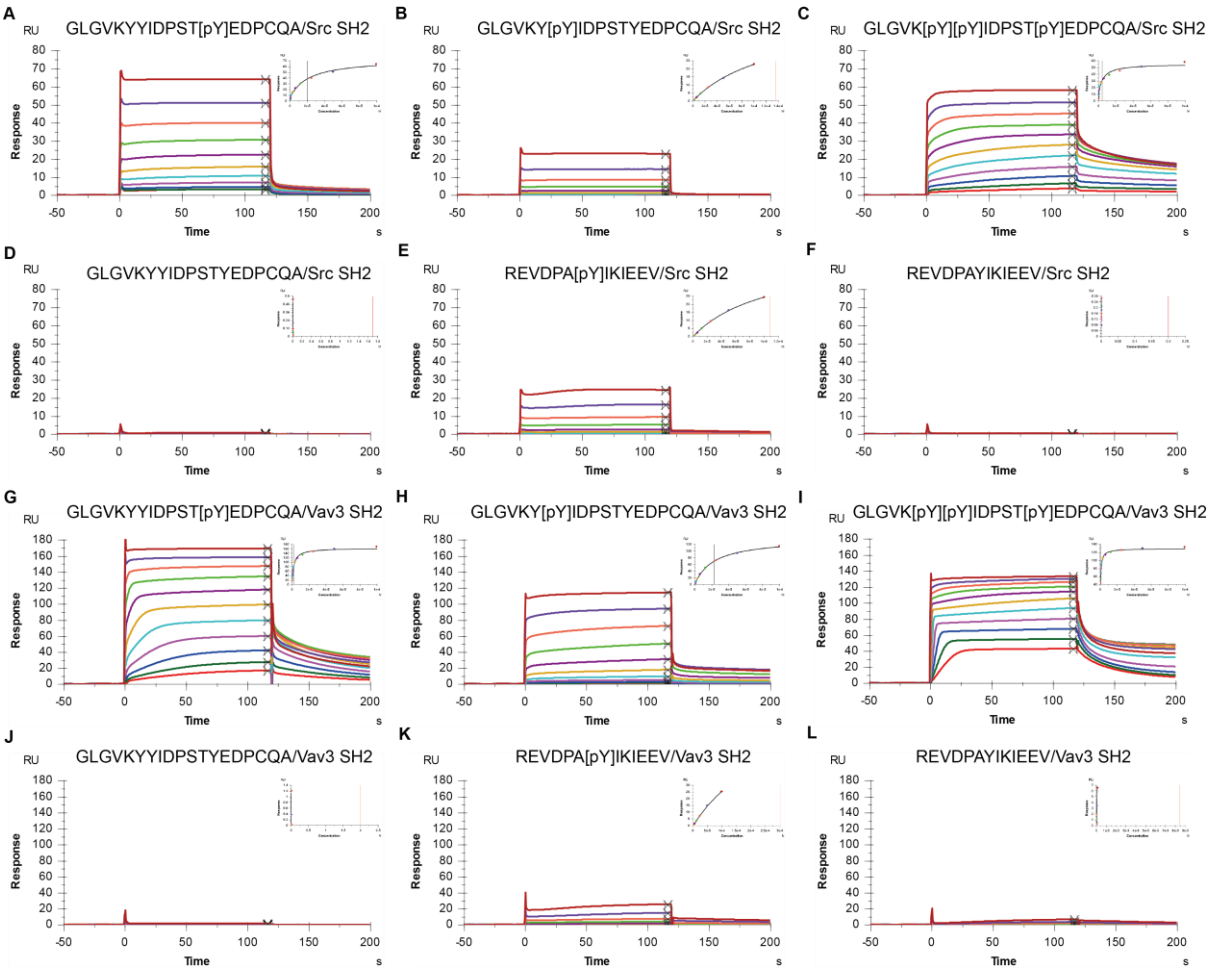

Supplementary Figure S6: Binding of Src and Vav3 SH2 domains to different phosphorylated EphB6 peptides measured by surface plasmon resonance (SPR).

Binding of the Src SH2 domain to pJX2 EphB6 peptide (A), pJX1 EphB6 peptide (B) and p644, pJX1 and pJX2 triphospho EphB6 peptide (C). (D) No binding was observed between the non-phosphorylated EphB6 peptide and Src SH2 domain. (E) p669 EphB6 peptide binding to Src SH2 domain. (F) No binding was observed between the non-phosphorylated peptide and Src SH2 domain. Binding of the Vav3 SH2 domain to pJX2 EphB6 peptide (G), pJX1 EphB6 peptide (H) and p644, pJX1 and pJX2 tri-phospho EphB6 peptide (I). (J) No binding was observed between the non-phosphorylated EphB6 peptide and Vav3 SH2 domain. (K) p669 EphB6 peptide binding to Vav3 SH2 domain. (L) No binding was observed between the non-phosphorylated peptide and Vav3 SH2 domain. Immobilisation levels of the Src SH2 and Vav3 SH2 domains on the CM5 chip were 1669.8 RU and 2017.6 RU, respectively.

Supplementary Table 1: SAXS data collection and analysis statistics

Data collection parameters	
Instrument	Australian Synchrotron SAXS/WAXS beamline
Detector	PILATUS3-2M (Dectris)
Wavelength (Å)	1.0332
Total q range ($Å^{-1}$)	0.005 – 0.5
Maximum flux at sample	8 x 10^{12} photons per second at 12 keV
Exposure time	Continuous 1 second frame measurements
Sample configuration	SEC-SAXS with co-flow
Temperature	12°C

Proteins	ΔN-EphB6	ΔN-EphB6 + AMPPNP	EphB6	EphA10
I(0) (cm^{-1}) (from Guinier analysis)	0.005 ± 7.1e-05	0.01 ± 6.4e-05	0.03 ± 18e-05	0.032 ± 26e-05
Rg (Å) (from Guinier analysis)	24.76 ± 0.60	25.04 ± 0.28	26.65 ± 0.24	30.19 ± 0.35
Rg (Å) (from P(r) analysis)	25.26 ± 0.42	25.56 ± 0.01	27.37 ± 0.03	31.55 ± 0.03
Dmax (Å)	82.26	89.52	100.43	113.40
Porod volume estimate ($Å^3$)	57290.60	55334.50	63183.40	71718.50
MW (from SAXSMoW)	34.1	40.6	48.5	54.8
MM (from volume of correlation, kDa)	34.7	36.8	41.7	45.4
MW (from sequence, kDa)	42.5	42.5	44.3	45.0

Software employed	
Primary data reduction	ScatterBrain (Australian Synchrotron)
Data processing	Primus (ATSAS)
Computation of model intensities	CRYSOL